Int. J. Electrochem. Sci., 17 **(2022)** Article Number: 220919, doi: 10.20964/2022.09.26

International Journal of
ELECTROCHEMICAL
SCIENCE
www.electrochemsci.org

Detection of hepatitis B virus DNA in human serum based on highly sensitive electrochemical sensor

Yan Wu, Ning Li, Shasha Xu, Xiaoyu Chong, Changgeng Zhang[*]

Clinical Laboratory, Hengshui People's Hospital, Hengshui, Heibei, 053000, PR China
[*]E-mail: zhangchanggengin@163.com

Received: 14 May 2022 / *Accepted:* 20 June 2022 / *Published:* 7 August 2022

The determination of specific DNA sequences in biological samples such as serum, organs, and body fluids is of great importance in biomedicine. Synthetic single-stranded DNA fragments of the Hepatitis B virus were immobilized as specific probes on the surface of gold electrodes using a self-assembled single-molecule membrane method. The electrode combined with the electroactive Hoechest 33258 constitutes the DNA electrochemical sensor. The film-forming conditions of self-assembled single-molecule membranes were explored during the immobilization of Hepatitis B specific DNA probes. The results showed that a probe concentration of 100 μg/mL and an immobilization time of 12 h was more favorable for the immobilization of the probe. We also explored the DNA immobilization and hybridization mechanism. We used a DNA electrochemical sensor for the qualitative and quantitative detection of standard concentrations of complementary DNA in solution. The results showed that the linear detection range could reach 0.05~1 μg/mL, and the limit of detection could reach 10 ng/mL when using the electrochemical sensor to detect standard DNA samples. On this basis, we have also successfully used DNA sensors for Hepatitis B virus detection serum.

Keywords: Electrochemical biosensor; DNA hybridization; Hepatitis B virus; Sensor; Hoechest33258

1. INTRODUCTION

The determination of specific DNA sequences in biological samples such as serum, organs, and body fluids is of great importance in biomedicine [1]. Its results can be used to identify and detect hereditary and infectious diseases. A DNA biosensor is a sensing device that converts the presence of target DNA into detectable signals such as electricity, light, and sound. It has become a cutting-edge topic in biosensors because it is fast, sensitive, and easy to operate compared with traditional methods of labeled gene technology [2–4]. The DNA electrochemical sensor consists of an electrode supporting a DNA fragment and an electroactive hybridization marker for detection. At the appropriate temperature, pH, and ionic strength, the probe molecules on the electrode surface can selectively hybridize with the

target sequence to form double-stranded DNA (dsDNA), resulting in a change in the electrode surface structure [5–7]. A hybridization marker can identify such structural differences before and after hybridization with electrical activity to detect target sequences or specific genes [8,9].

Although Au electrode as the basic electrode has been used for electrochemical research, the application of modified Au electrode is far less common than carbon electrode. Wang et al. [10] mentioned in the determination of a short DNA sequence associated with human immunodeficiency virus type I that if a gold disc electrode was used for membrane assembly for hybridization assays, its signal-to-noise ratio was reduced to that of a carbon paste electrode. However, the conventional probe assembly time is too long. Suppose the traditional method of immobilizing molecules directly on the Au electrode surface is changed. The self-assembled deuterium single-molecule film technique is adopted to modify the electrode at the molecular level to make the electrode surface functionalized. In that case, the probe assembly time can be shortened [11,12].

A self-assembled single-molecule membrane can be formed on the surface of the Au electrode with aminoethyl mercaptan [13]. Then, using water-soluble carbonated diimine as a coupling activator, the phosphate group at the 5' end of ssDNA is covalently bound to the activated amino group on the electrode surface in the form of a phosphorylamino vinegar bond, which can while forming an ssDNA monomolecular layer on the gold surface [14]. In addition, the immobilization of ssDNA with a thiohexyl group at the 5' end on the cleaned gold electrode allows further reduction of probe immobilization time. The literature also reported that an ordered layer of streptavidin biphosphate membranes containing metal-centered Al^{3+} ions can strongly interact with negatively charged DNA strands to immobilize DNA on the electrode surface through an ordered adsorption and reaction step [15].

Viral Hepatitis B (HBV) is one of the major diseases affecting human health today. Nearly one-third of the world's population is infected with HBV, and one in five of these patients will develop chronic HBV carriers. If chronic viral hepatitis B is not effectively controlled, it can lead to cirrhosis and even severe complications such as liver cancer, leading to death [16–20]. Therefore, timely and effective prevention of hepatitis has become a significant public health issue worldwide.

This paper uses the genetic detection of the Hepatitis B virus as a model to design gene probes with conventional Au electrodes as substrate electrodes. Then, we investigated the self-assembled single-molecule membrane technology and constructed DNA electrochemical sensors. We optimized each sensor's performance to establish a DNA electrochemical sensor for rapidly detecting the Hepatitis B virus. This work lays the foundation for developing immobilization techniques and assays for detecting HBV-DNA with high specificity, good sensitivity, long life, and low cost.

2. EXPERIMENTAL

2.1. Reagents

Tris powder, mercaptohexanol, Hoechst 33258, and Daunorubicin were purchased from Sigma. DNA extracts were purchased from Shenzhen Piki Bioengineering Co. All other regents were analytical grade and purchased from Shanghai Sinopharm Reagent Co. Piranha solution (98% concentrated sulfuric

acid: 30% hydrogen peroxide = 3:1) is used as a renewal treatment for gold electrode surfaces. 5 mM $Fe(CN)_6^{3-}/Fe(CN)_6^{4-}$+ 0.01 M KCl was prepared by dissolving 0.3293 g $K_3Fe(CN)_6$, 0.4224 g $K_4Fe(CN)_6$ and 0.1491 g KCl in 200 mL water. 10 mM Tris-HCl + 0.1 M NaCl was prepared by dissolving 0.9692 g Tris powder, 3.8760 g NaCl into 750 mL water and adjusted the pH to 80 using 0.1 M HCl and add water to 800 mL. 10 mM Tris-HCl + 1 mM EDTA was prepared by dissolving 0.1211 g Tris powder and 0.03722 g EDTA in 90 mL water. The pH was adjusted by 0.1 M HCl to 8 and added to 100 mL using water. 0.1 M NaH_2PO_4-Na_2HPO_4 solution was prepared by dissolving 1.56 g NaH_2PO_4 and 3.5814 g NaH_2PO_4 into 90 mL water. 2XSSC solution was prepared by dissolving 0.8824 g sodium citrate and 1.755 g NaCl into 100 mL water. 0.1 mM Hoechst33258 was prepared by dissolving 0.0005 g Hoechst33258 into 10 mL Tris-HCl+ 1 mM EDTA solution.

Single-stranded DNA probe S1 labeled with deucalcitol at the 5' end.

5’-HS-$(CH_2)_6$-GGGTATACATTTGAACCCCAAT-3’

Single-stranded DNA that is fully complementary to the synthetic probe S2:

5’-ATTGGGGTTCAAATGTATACCC-3’

Single-stranded DNA with one base mismatch to the synthetic probe S3:

5’-ATTGGGGTTCAAATGTCTACCC-3’

Preparation of human serum: Add 100 μL of fresh plasma into a 0.5 mL centrifuge tube, add 100 μL of DNA extract, centrifuge at 13000 rmp for 10 min and discard the supernatant. Add another 25 μL of DNA extract and centrifuge at 2000 rmp for 10 s. Then, the solution was treated with boiling water at 100^{o}C for 10 min and centrifuged at 13000 rmp for 10 min, and the supernatant was retained for the assay.

2.2. Electrode modification

The Au electrode was pretreated before each probe assembly to remove the organic impurities on the surface. The Au electrode is soaked with Piranha solution for 30 min, cleaned with acetone, anhydrous ethanol and water in turn, and then polished with 0.05 μm particle size Al_2O_3 abrasive pad. Finally, ultrasonic cleaning for 3 min, dry the gold surface with N_2.

The Au electrode was immersed in a fixative solution containing 0.04 mL of 100 μg/mL DNA S1 and placed at 4^{o}C for 12 h to obtain the single-stranded DNA modified electrode (MCH/Au electrode). The electrode surface was sequentially washed with 10 mM Tris-0.1 M NaCl and water to remove unassembled DNA (HS-ssDNA/Au).

The HS-ssDNA/Au was immersed in 100 μM Hoechst33258 solution for 10 min. After removing the electrode, the electrode was washed with 10 mM Tris-HCl+0.1 M NaCl and water to remove the excess hybridization marker.

50 μg/mL of complementary ssDNA (S2) was prepared with Tris buffer solution, and then it was diluted into different gradients with 2XSSC buffer solution, respectively. The HS-ssDNA/Au modified electrode was placed in a specific concentration of complementary single-stranded DNA in a 2XSSC buffer solution for 90 min hybridization reaction. The electrode was washed with 10 mM Tris-HCl + 0.1 M NaCl and water (denoted as HS-dsDNA/Au).

50 μg/mL of single-base mismatched ssDNA (S3) was configured with Tris buffer solution and then diluted to 1 μg/mL and 10 ng/mL with 2XSSC buffer solution. The prepared HS-ssDNA/Au electrode was placed in a specific concentration of single-base mismatched ssDNA in a 2XSSC buffer solution, and DNA hybridization was performed at room temperature for 90 min. Then the electrode was washed with 10 mM Tris-HCl + 0.1 M NaCl and water.

All electrochemical experiments were performed on a CHI 760E point electrochemical workstation. The scanning mode was not linear voltammetric scanning. The buffer solution was 0.1 M PBS. Cyclic voltammetry (CV) and linear sweep voltammetry (LSV) has been used for analysis. The scanning speed was 20-100 mV/s.

3. RESULTS AND DISCUSSION

Molecular self-assembly is a class of molecular aggregates or supramolecular structures with a well-defined and stable structure and a specific function or property formed by the spontaneous combination of molecules through non-covalent interactions under equilibrium conditions. The analysis of biomolecular self-assembly systems shows that self-assembly is driven by weak and reversible non-covalent interactions, such as hydrogen bonding, π-π interactions, etc. At the same time, the structural stability and integrity of the self-assembled system are maintained by these interactions non-covalent interactions [21–23]. Self-assembled monomolecular membrane (SAM) refers to the natural formation of highly ordered monomolecular layers on a solid surface based on the self-assembly of molecules. HS-ssDNA can form self-assembled films on the surface of gold electrodes due to the strong chemical binding of sulfhydryl groups to the substrate material and the oriented arrangement of polymethylene chains. Therefore, to verify the self-assembly of single-stranded DNA modification [24–26], we examined the voltammetric signals of bare gold electrodes and HS-ssDNA/Au electrodes in 0.5 M KCl in the range of 0~-1.1 V (Figure 1A). It was found that the current intensity of peak 1 of the bare Au electrode was very high before the bottom solution was deoxygenated by nitrogen and decreased significantly after the de-oxygenation, which indicates that the generation of peak 1 is related to oxygen. The HS-ssDNA/Au electrode under the same conditions has essentially no peaks 1, which is due to the formation of a self-assembled film on the electrode surface that prevents the electron transfer of oxygen on the electrode surface. Meanwhile, the HS-ssDNA/Au electrode produced the characteristic reduction peak of Au-SR around -0.9 V (peak 2), indicating that the sulfhydryl-hexyl-modified ssDNA has been immobilized on the gold electrode surface by self-assembly. Figure 1B shows the continuous scan of the HS-ssDNA/Au electrode. The peak 2 around -0.9 V gradually decreases as the number of scans increases, and by the time the scan proceeds to the fifth, the peak current is already small. Meanwhile, peak 1 gradually increased, indicating that with the increase in the number of scans, the HS-ssDNA modified on the surface of the Au electrode was gradually shed, leading to the gradual and obvious electron transfer of oxygen on the gold surface [27]. It can be seen that the stability of DNA-modified electrodes is poor under the applied negative voltage, and the use of DNA-modified electrodes in the more negative voltage range should be avoided.

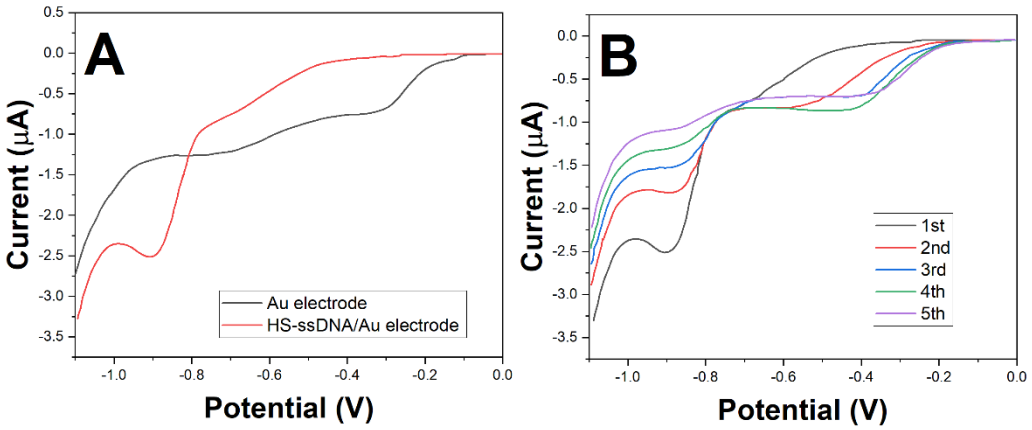

Figure 1. (A) LSV of bare Au electrode and HS-ssDNA/Au electrode. (B) LSV of HS-ssDNA/Au electrode with five successive scans. Scan rate: 50 mV/s. Electrolyte: 0.5 M KCl.

Long-chain thiol self-assembled membranes are almost impermeable to inorganic ions. In contrast, short-chain thiol self-assembled membranes are permeable to inorganic ions due to their uneven and dense molecular arrangement [28,29]. We examined the hindering effect of HS-ssDNA/Au self-assembled membrane on electron transfer with 5 mM $Fe(CN)_6^{3-}$/$Fe(CN)_6^{4-}$+0.01 M KCl (Figure 2). The MCH/Au electrode obtained after electrode modification by mercaptohexanol forms a dense film on the surface, hindering the electron transport of iron ions on the electrode surface to a certain extent. When the electrode was self-assembled with ssDNA modified by mercaptohexanol, HS-ssDNA/Au electrode was obtained. Since the 22-base DNA fragment is several times the length of the mercaptohexol molecule, electron transport of iron ions at the electrode surface is more complicated, making the difference in peak potential larger and the peak current smaller.

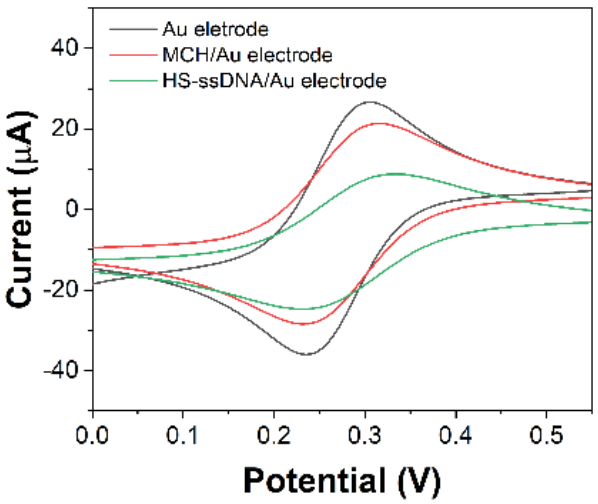

Figure 2. CV of bare Au electrode, MCH/Au electrode and HS-ssDNA/Au electrode in 5 mM $Fe(CN)_6^{3-}$/$Fe(CN)_6^{4-}$+0.01 M KCl. Scan rate: 50 mV/s.

The Au electrode was placed in 100 μg/mL of ss-DNA and self-assembled at 4°C at different times to observe its electrochemical response signal in 0.5 M KCl, and the results are shown in Figure 3A. In 30-240 min, the amount of self-assembled HS-ssDNA on the Au electrode surface increased continuously. After 240 min, this trend slowed down significantly, indicating that the amount of self-assembled HS-ssDNA on the electrode surface had saturated. However, the figure does not reflect the slower surface recombination process of HS-ssDNA after rapid adsorption on the electrode surface. Moreover, if the electrochemical sensor made by self-assembly 240 min is used to detect the complementary sequence DNA, only a weak response signal can be observed. This indicates that HS-ssDNA does not form a complete ordered monomolecular layer in a short time after rapid adsorption on the electrode surface [30,31]. Therefore, choosing the appropriate self-assembly time is necessary to obtain the best response value.

We examined the effect of self-assembly time on the oxidation peak current (Figure 3B). The self-assembly time was less than 8 h, and the response value obtained was relatively small. The response value was only gradually stabilized after 10 h, indicating that the self-assembled HS-ssDNA on the electrode surface only completed the slow surface recombination process at this time. Then the hybridization with the complementary strand was achieved [32]. After 12 h, the response value o still increased, but the magnitude was small. Combining the above experimental results, we choose the self-assembly time of the electrode as 12 h.

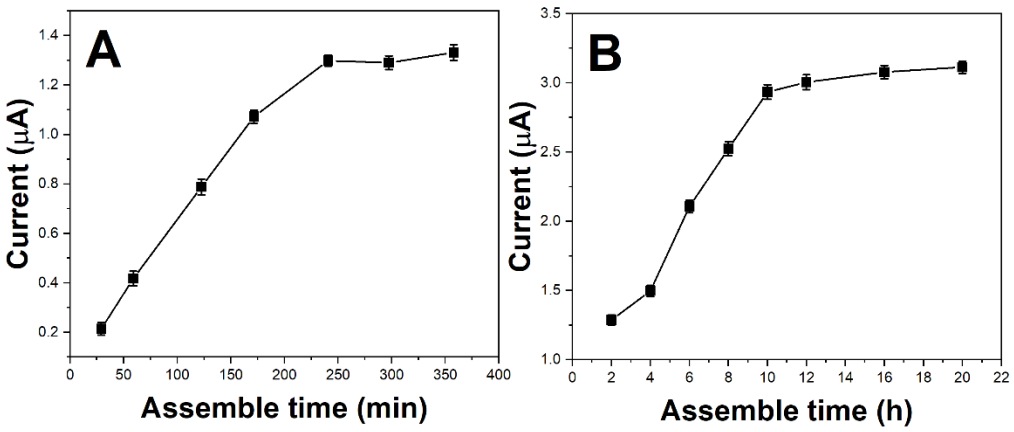

Figure 3. Effect of (A) assemble time of HS-ssDNA and (B) assemble time of oxidation peak current. Scan rate: 50 mV/s. Electrolyte: 0.5 M KCl.

HS-ssDNA is modified on the electrode surface as a probe, so the stability of the HS-ssDNA electrode directly affects the performance of DNA electrochemical sensors [33]. We examined the stability of the HS-ssDNA electrode in the range of 0.1-0.8 V by the oxidation peak current. Special attention is paid to re-binding and cleaning the electrode after each scan since the electrode is completely dislodged after one linear voltammetric scan. The experiments showed that the peak current response value was small when the first voltammetric scan was performed. After the first activation, the oxidation

peak current o was stable at the second four scans and then increased with the number of scans. The peak current decreases significantly after five times. The peak current disappears, indicating that the HS-ssDNA on the electrode is shed [34]. In summary, when examining the response value on HS-ssDNA, we chose the peak current value obtained at the second scan. Furthermore, the peak current value obtained from the first scan when the sensor was embedded after hybridization was selected as the response value on HS-ssDNA.

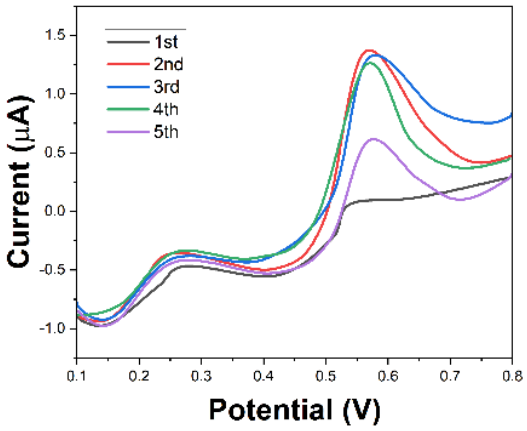

Figure 4. Effect of scan times of peak current using HS-ssDNA/Au electrode. Scan rate: 50 mV/s. Electrolyte: 0.5 M KCl.

The sensor used in DNA electrochemical sensors are a class of electroactive compounds that can interact with ssDNA and dsDNA. When combined with DNA, a reversible redox reaction can occur when electrons are exchanged with DNA. DNA completes the electrochemical reaction process through remote electron transfer so that the electrode can exchange electrons with the electrode [35–37]. The current study identified Daunorubicin and Hoechst 33258 as two indicators with high specificity. Daunorubicin binds differently to dsDNA and ssDNA, so its oxidation peak potential on the dsDNA-modified electrode has a more apparent positive shift than on the ssDNA-modified electrode. However, as the complementary chain concentration decreased, especially for the ng-level complementary chains to be measured, the potential difference between Daunorubicin at the single and double chain modified electrodes decreased significantly. Hoechst 33258, as an electroactive dye, can produce an irreversible oxidation peak current at a lower potential at an Au electrode. Compared with Daunorubicin, Hoechst33258 binds dsDNA more selectively and can maintain good specificity at lower concentrations of the complementary strand to be tested.

The Hoechst 33258 produces a weak signal for bare electrodes due to physical adsorption. For HS-ssDNA/Au, the electrostatic binding interaction between Hoechst 33258 and ssDNA resulted in an oxidation peak signal. For dsDNA, Hoechst33258 can be embedded in the base pairs of the double helix structure formed by dsDNA, forming a dsDNA-Hoechst33258 layer on the electrode surface resulting in a strong oxidation peak signal [38,39]. Also, similar to daunorubicin, Hoechst 33258 was more stable

in its embedding with dsDNA than in its electrostatic binding with ssDNA, thus producing a corresponding positive shift in the oxidation peak potential [40–42]. However, the magnitude of the positive shift is smaller than that of daunorubicin. Therefore, the oxidation peak currents of Hoechst33258 on HS-ssDNA/Au and HS-dsDNA/Au electrodes are generally compared to determine whether the DNA probe molecules on the electrode surface are hybridized with the target sequence molecules. Voltammetric signals of Hoechst33258 on DNA modified electrodes are shown in Figure 5.

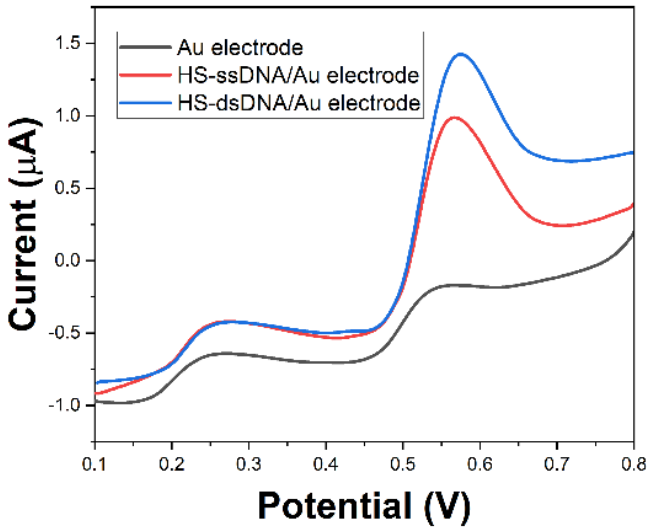

Figure 5. The different peak current of Hoechst 33258 on bare Au electrode, HS-ssDNA/Au electrode and HS-dsDNA/Au electrode. Scan rate: 50 mV/s. Electrolyte: 0.5 M KCl.

A series of parameters were optimized. Five HS-ssDNA/Au electrodes were prepared and hybridized with 1 μg/mL of complementary DNA solution for 90 min, and after removal and cleaning, marker embedding was performed. The relationship between the action time and the response signal was obtained in Figure 6A. When the marker embedding time was less than 5 min, the electrochemical response increased rapidly at any time. At 5-10 minutes, the peak current value increases slowly. At 10-15 minutes, the peak current value is stable. Therefore, we choose 10 minutes as the time of action in our experiments.

The marker can interact with dsDNA through embedded binding, electrostatic binding, and ssDNA interaction to produce a specific electrochemical response. Our experiments also found that even for bare Au electrodes, the marker produces a particular signal due to physical adsorption. Therefore, for both HS-ssDNA/Au and HS-dsDNA/Au electrodes, the electrode surface should be repeatedly drenched with 10 mM Tris-HCl+0.1 M NaCl solution after the marker interacts with it to minimize the non-specific adsorption of the marker. We examined the effect of buffer drenching time on the oxidation peak current of Hoechst 33258 at HS-ssDNA/Au and HS-dsDNA/Au electrodes, respectively, and the results are shown in Figure 6B. For both HS-ssDNA/Au and HS-dsDNA/Au electrodes, the peak current of the marker generated by non-specific adsorption was reduced to different degrees after buffer

drenching [43]. The response signal obtained with insufficient drenching time was large. Too long a drench time prolongs the operation time and leads to the loss of the marker embedded in the double helix DNA of the modified electrode. Therefore, after the modified electrode interacted with the marker, we chose a drench time of 10 min for the buffer.

The essence of the hybridization of DNA molecules is to use nucleic acid molecules' denaturing and complexing properties to form dsDNA fragments of different origins in a base-complementary relationship. The presence of monovalent cations such as Na^+ can increase the rate of heterologous hybrid double-stranded generation. The principle is that Na^+ can mask the negatively charged phosphate backbone, affecting the base-pairing interactions between the target gene and the probe molecule. Therefore, the variation of NaCl concentration in the hybridization buffer greatly influences the hybridization signal [44]. We examined the hybridization effect of 0.125 μg/mL of ssDNA entirely complementary to the immobilized probe at different NaCl concentrations by the response signal. As shown in Figure 6C, the hybridization detection signal of DNA decreased sharply at low NaCl concentrations but increased when NaCl concentration was increased. However, the rise became slow after 0.2 M. When the NaCl concentration was between 0.2-0.4 M, the current was several maximum. After 0.4 M, the current showed a decreasing trend.

The hybridization temperature of DNA sequences is related to its denaturation temperature. We examined the hybridization of the probe with 0.25 μg/mL of complementary DNA at four temperatures of 25℃, 35℃, 45℃, and 60℃ (Figure 6D). With the increase of hybridization time, the amount of hybridization tended to rise and gradually reached the maximum value, after which it stopped and no longer rose. The higher the temperature, the shorter the time for the hybridization amount to reach the maximum. This is because, at higher temperatures, the DNA molecules move faster, and the hybridization equilibrium is reached quickly [45]. However, another effect of temperature on the amount of hybridization is that the maximum amount of hybridization gradually decreases as the temperature of hybridization increases. This phenomenon may be because the hybridization is solid-liquid heterogeneous hybridization at this time, and the stability of the modified electrode at higher temperatures needs to be considered. Since the hybridization occurs at the solid-liquid junction, the stability of the electrode becomes less stable as the temperature rises, and the denaturation of the DNA double-stranded molecules after hybridization is accelerated, so the absolute hybridization amount decreases. 45℃, although the hybridization speed is fast when the hybridization is carried out to a certain extent and then extended the hybridization time, the signal no longer increases and decreases rapidly. This indicates that the denaturation of the double chain is dominant at this time, which affects the continuation of the hybridization reaction. Therefore, we chose to hybridize at 25℃ for 90 min.

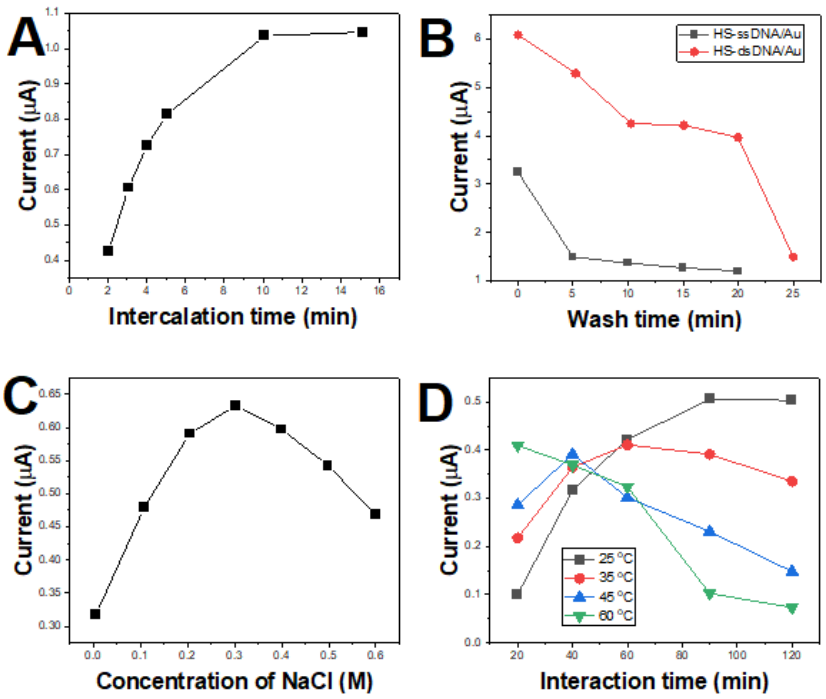

Figure 6. The effect of (A) intercalation time, (B) wash time of buffer solution, (C) concentration of Na^+ and (D) temperature on the current response of HS-dsDNA/Au electrode. Scan rate: 50 mV/s. Electrolyte: 0.5 M KCl.

In the range of 0.05-1 μg/mL, a linear relationship was observed between the peak current response values before and after the hybridization of the complementary DNA with the modified electrodes at different mass concentrations (Figure 7). Although there is no good linearity for complementary strand mass concentrations below 0.05 μg/mL, an excellent voltammetric signal can be observed and shows good specificity. At complementary strand mass concentrations below 10 ng/mL, the voltammetric signal can be observed at HS-ssDNA/Au and HS-dsDNA/Au electrodes. However, the presence of single-base mismatched DNA may cause significant errors.

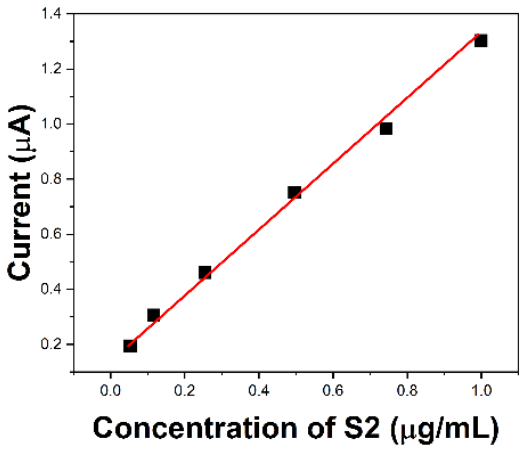

Figure 7. The linear relation ship between the complementary DNA solution of different concentration and current.

Ten HS-ssDNA/Au electrodes were used with 0.5 μg/mL of complementary DNA (S2) solution, and the response values are shown in Table 1. It can be seen that the DNA electrochemical sensor has good reproducibility for a specific concentration of complementary DNA solution. When the complementary strand concentration is equal to 10 ng/mL, the current value is greater than 3 times the standard deviation of 0.026 μA. 10 ng/mL is used as the detection limit of the sensor.

Table 1. Reproducibility of the electrochemical DNA sensor.

Test	**1**	**2**	**3**	**4**	**5**	**6**	**7**	**8**	**9**	**10**
Current (μA)	0.771	0.764	0.760	0.765	0.759	0.762	0.780	0.774	0.765	0.762

The HS-ssDNA/Au electrode was used with two concentrations of complementary DNA (S2) solution and single-base mismatch DNA (S3) solution at 1 μg/mL and 10 ng/mL, respectively, to examine the voltammetric signal, and the results are shown in Table 2. When the single base mismatch solution concentration was 100 times the complementary concentration, the response signal obtained was about half of that of the complementary DNA solution. At the same concentration, the response signal caused by the single-base mismatched DNA sequence only accounts for about 3% of the entirely complementary sequence. Therefore, within a specific concentration range, the DNA electrochemical sensor is able to distinguish well between complementary DNA sequences and single-base mismatched DNA sequences.

Table 2. The current response of the intercalator when the DNA sensor interacted with un-matched DNA.

DNA concentration	**S2**	**S3**
1 μg/mL	0.901	0.021
10 ng/mL	0.051	0.009

Figure 8 shows the sensor's detection of serum samples containing the Hepatitis B virus. The LSV in the figure includes the signal generated by the sensor probe, the signal generated after hybridization of the processed serum sample with the DNA sensor probe, and the signal after hybridization with the synthetic probe complementary to S2. It can be seen that when the serum contains the Hepatitis B virus, the current is 0.908 μA, which is similar to the current value and peak pattern produced by S2. The synthesized complementary sequence has only 22 bases, and it has a small spatial site resistance in binding to the electrochemical sensor. In contrast, the Hepatitis B virus in serum, although the most minor double-stranded DNA virus known to infect humans, has several thousand base fragments [46]. Its length limits it in the hybridization with the sensor. The potential spatial resistance is larger, making the hybridization rate decrease, thus leading to a relative decrease in the response signal

[47]. Again since the Hepatitis B virus in serum has thousands of base fragments, once it has achieved hybridization with the probe on the sensor, the amount of adsorption is much greater than in the case of tens of base fragments. Therefore, the concentration of hepatitis B virus in the serum samples fell exactly within the linear range of our study. Table 3 shows the comparison of the actual serum samples detected using the DNA sensor and fluorescent PCR. As can be seen from the table, the DNA electrochemical sensor detected all PCR positives, and the high number of viruses in the fluorescence PCR analysis results was associated with approximately high current values in the sensor analysis results. For regular human blood oxygen, the current observed with the sensor is much smaller than that of the sample [48,49]. Therefore, DNA electrochemical sensors can be used to detect the Hepatitis B virus in serum.

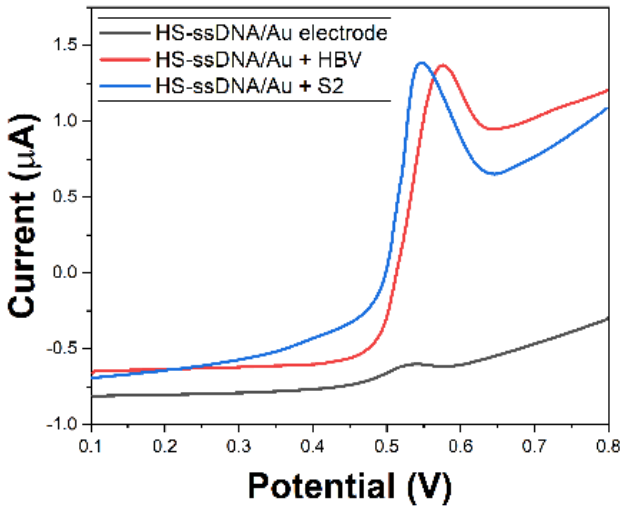

Figure 8. LSV of HS-ssDNA/Au, HS-ssDNA/Au interacted with serum sample with Hepatitis B virus, HS-ssDNA/Au interacted with S2.

Table 3. Comparison of fluorescence PCR and DNA electrochemical sensor towards Hepatitis B virus in serum samples.

Sample	**1**	**2**	**3**	**4**	**5**
Fluorescence PCR (copies/L)	6.15×10^8	7.82×10^6	4.95×10^6	3.55×10^5	4.04×10^4
DNA sensor (μA)	0.907	0.644	0.557	0.481	0.396

4. CONCLUSION

This work used an Au electrode as a substrate to immobilize a specific DNA probe from a designed Hepatitis B virus DNA sequence using a self-assembled single-molecule membrane method.

This allowed the fabrication of a DNA electrochemical sensor for the quantitative and qualitative detection of standard concentrations of complementary single strands and was performed on clinically obtained serum samples of Hepatitis B virus. We optimized the conditions for hybridization of the DNA electrochemical sensor in terms of temperature and ionic strength. The results show that the lower temperature takes longer time for hybridization to reach equilibrium, but the amount of hybridization is large. The best hybridization effect was achieved when the concentration of NaCl in the hybridization buffer was 0.3 M. Hoechst 33258 has high selectivity for double-stranded DNA and can generate a high density of oxidation peak current at a lower potential, which is an ideal electroactive marker. A series of complementary single-stranded DNAs at different concentrations were assayed by hybridization using the developed DNA electrochemical sensor.

References

1. W.H. Pope, D. Jacobs-Sera, *Bacteriophages* (2018) 217.
2. G. Gong, C. Dan, S. Xiao, W. Guo, P. Huang, Y. Xiong, J. Wu, Y. He, J. Zhang, X. Li, *GigaScience*, 7 (2018) 120.
3. L. Chalupowicz, A. Dombrovsky, V. Gaba, N. Luria, M. Reuven, A. Beerman, O. Lachman, O. Dror, G. Nissan, S. Manulis-Sasson, *Plant Pathology*, 68 (2019) 229.
4. F.-F. Wu, Y. Zhou, H. Zhang, R. Yuan, Y.-Q. Chai, *Analytical Chemistry*, 90 (2018) 2263.
5. S.-Q. Zhang, K.-Y. Ma, A.A. Schonnesen, M. Zhang, C. He, E. Sun, C.M. Williams, W. Jia, N. Jiang, *Nature Biotechnology*, 36 (2018) 1156.
6. Y. Yang, K.E. Niehaus, T.M. Walker, Z. Iqbal, A.S. Walker, D.J. Wilson, T.E. Peto, D.W. Crook, E.G. Smith, T. Zhu, *Bioinformatics*, 34 (2018) 1666.
7. J. Naue, T. Sänger, H.C. Hoefsloot, S. Lutz-Bonengel, A.D. Kloosterman, P.J. Verschure, *Forensic Science International: Genetics*, 36 (2018) 152.
8. R. O'Hara, E. Tedone, A. Ludlow, E. Huang, B. Arosio, D. Mari, J.W. Shay, *Genome Research*, 29 (2019) 1878.
9. B. Bo, T. Zhang, Y. Jiang, H. Cui, P. Miao, *Analytical Chemistry*, 90 (2018) 2395.
10. J. Wang, G. Rivas, D. Luo, X. Cai, F.S. Valera, N. Dontha, *Analytical Chemistry*, 68 (1996) 4365.
11. X. Qian, S. Tan, Z. Li, Q. Qu, L. Li, L. Yang, *Biosensors and Bioelectronics*, 153 (2020) 112051.
12. T. Lee, G.H. Kim, S.M. Kim, K. Hong, Y. Kim, C. Park, H. Sohn, J. Min, *Colloids and Surfaces B: Biointerfaces*, 182 (2019) 110341.
13. N.K. Mogha, V. Sahu, R.K. Sharma, D.T. Masram, *Journal of Materials Chemistry B*, 6 (2018) 5181.
14. T.M. Herne, M.J. Tarlov, *Journal of the American Chemical Society*, 119 (1997) 8916–8920.
15. H. Pu, X. Xie, D.-W. Sun, Q. Wei, Y. Jiang, *Talanta*, 195 (2019) 419.
16. I. Lazarevic, A. Banko, D. Miljanovic, M. Cupic, *Viruses*, 11 (2019) 778.
17. J. Kim, S.Y. Oh, S. Shukla, S.B. Hong, N.S. Heo, V.K. Bajpai, H.S. Chun, C.-H. Jo, B.G. Choi, Y.S. Huh, *Biosensors and Bioelectronics*, 107 (2018) 118.
18. C. Srisomwat, P. Teengam, N. Chuaypen, P. Tangkijvanich, T. Vilaivan, O. Chailapakul, *Sensors and Actuators B: Chemical*, 316 (2020) 128077.
19. M. Shariati, *Biosensors and Bioelectronics*, 105 (2018) 58
20. S.A. Galel, T.L. Simon, P.C. Williamson, J.P. AuBuchon, D.A. Waxman, Y. Erickson, R. Bertuzis, J.R. Duncan, K. Malhotra, J. Vaks, *Transfusion*, 58 (2018) 649.

21. C. Srisomwat, A. Yakoh, N. Chuaypen, P. Tangkijvanich, T. Vilaivan, O. Chailapakul, *Analytical Chemistry*, 93 (2020) 2879.
22. H. Karimi-Maleh, Y. Orooji, F. Karimi, M. Alizadeh, M. Baghayeri, J. Rouhi, S. Tajik, H. Beitollahi, S. Agarwal, V.K. Gupta, *Biosensors and Bioelectronics*, 184 (2021) 113252.
23. H. Karimi-Maleh, A. Khataee, F. Karimi, M. Baghayeri, L. Fu, J. Rouhi, C. Karaman, O. Karaman, R. Boukherroub, *Chemosphere*, 291 (2021) 132928.
24. S. Boonkaew, A. Yakoh, N. Chuaypen, P. Tangkijvanich, S. Rengpipat, W. Siangproh, O. Chailapakul, *Biosensors and Bioelectronics*, 193 (2021) 113543.
25. P. Kannan, P. Subramanian, T. Maiyalagan, Z. Jiang, *Analytical Chemistry*, 91 (2019) 5824.
26. Z. Zhang, M. Peng, D. Li, J. Yao, Y. Li, B. Wu, L. Wang, Z. Xu, *Frontiers in Chemistry*, 9 (2021) 702.
27. H. Karimi-Maleh, F. Karimi, L. Fu, A.L. Sanati, M. Alizadeh, C. Karaman, Y. Orooji, *Journal of Hazardous Materials*, 423 (2022) 127058.
28. N.Y. Jayanath, L.T. Nguyen, T.T. Vu, L. Dai Tran, *RSC Advances*, 8 (2018) 34954.
29. M.R. de Eguilaz, L.R. Cumba, R.J. Forster, *Electrochemistry Communications*, 116 (2020) 106762.
30. F. Zhao, Y. Bai, L. Cao, G. Han, C. Fang, S. Wei, Z. Chen, *Journal of Electroanalytical Chemistry*, 867 (2020) 114184.
31. H. Karimi-Maleh, M. Alizadeh, Y. Orooji, F. Karimi, M. Baghayeri, J. Rouhi, S. Tajik, H. Beitollahi, S. Agarwal, V.K. Gupta, S. Rajendran, S. Rostamnia, L. Fu, F. Saberi-Movahed, S. Malekmohammadi, *Ind. Eng. Chem. Res.*, 60 (2021) 816.
32. S. Yan, Y. Yue, L. Zeng, L. Su, M. Hao, W. Zhang, X. Wang, *Frontiers in Chemistry*, 9 (2021) 220.
33. A.M. Ichzan, S.-H. Hwang, H. Cho, C. San Fang, S. Park, G. Kim, J. Kim, P. Nandhakumar, B. Yu, S. Jon, *Biosensors and Bioelectronics*, 179 (2021) 113065.
34. H. Karimi-Maleh, H. Beitollahi, P.S. Kumar, S. Tajik, P.M. Jahani, F. Karimi, C. Karaman, Y. Vasseghian, M. Baghayeri, J. Rouhi, *Food and Chemical Toxicology* (2022) 112961.
35. J. Liu, T. Yang, J. Xu, Y. Sun, *Frontiers in Chemistry*, 9 (2021) 488.
36. Y. Zheng, D. Wang, X. Li, Z. Wang, Q. Zhou, L. Fu, Y. Yin, D. Creech, *Biosensors*, 11 (2021) 403.
37. D. Wang, D. Li, L. Fu, Y. Zheng, Y. Gu, F. Chen, S. Zhao, *Sensors*, 21 (2021) 8216.
38. X. Lin, X. Lian, B. Luo, X.-C. Huang, *Inorganic Chemistry Communications*, 119 (2020) 108095.
39. E.K.G. Trindade, R.F. Dutra, *Colloids and Surfaces B: Biointerfaces*, 172 (2018) 272.
40. X. Li, T. Liu, Y. Zhang, X. Ni, M.N. Hossain, X. Chen, H. Huang, H.-B. Kraatz, *Talanta*, 221 (2021) 121459.
41. H. Karimi-Maleh, A. Ayati, S. Ghanbari, Y. Orooji, B. Tanhaei, F. Karimi, M. Alizadeh, J. Rouhi, L. Fu, M. Sillanpää, *Journal of Molecular Liquids*, 329 (2021) 115062.
42. H. Karimi-Maleh, A. Ayati, R. Davoodi, B. Tanhaei, F. Karimi, S. Malekmohammadi, Y. Orooji, L. Fu, M. Sillanpää, *Journal of Cleaner Production*, 291 (2021) 125880.
43. L.C. Brazaca, P.L. dos Santos, P.R. de Oliveira, D.P. Rocha, J.S. Stefano, C. Kalinke, R.A. Abarza Muñoz, J.A. Bonacin, B.C. Janegitz, E. Carrilho, *Analytica Chimica Acta*, 1159 (2021) 338384.
44. D.A. Oliveira, J.V. Silva, J.M.R. Flauzino, H.S. Sousa, A.C.H. Castro, A.C.R. Moço, M.M.C.N. Soares, J.M. Madurro, A.G. Brito-Madurro, *Journal of Electroanalytical Chemistry*, 844 (2019) 6.
45. M.Z.H. Khan, M.R. Hasan, S.I. Hossain, M.S. Ahommed, M. Daizy, *Biosensors and Bioelectronics*, 166 (2020) 112431.
46. D.H. Mohsin, M.S. Mashkour, F. Fatemi, *Chemical Papers*, 75 (2021) 279.
47. J. P. de Campos da Costa, W. B. Bastos, P. I. da Costa, M. A. Zaghete, E. Longo, J. P. Carmo, *IEEE Sensors Journal*, 19 (2019) 10701.
48. W. Preidel, J. Rao, K. Mund, O. Schunck, E. David, *Sensors and Actuators B: Chemical*, 28 (1995) 71.

49. L. Rivas, S. Dulay, S. Miserere, L. Pla, S.B. Marin, J. Parra, E. Eixarch, E. Gratacós, M. Illa, M. Mir, *Biosensors and Bioelectronics*, 153 (2020) 112028.